RESEARCH ARTICLE
doi: 10.2306/scienceasia1513-1874.2026.051

ScienceAsia 52 (3): 2026: ID 2026051: **1–8**

Radiation protection of polysaccharides from *Stropharia rugosoannulata*

Xiaofei Liang[a,†], **Chen Ruan**[a,†], **Chenxi Wu**[a], **Huiguo Xie**[a], **Lujie Yang**[a], **Wei Wu**[b], **Yingying Zhang**[b,*], **Xinhong Wang**[c,*]

[a] School of Pharmacy, Shandong University of traditional Chinese Medicine, Jinan 250355 China
[b] School of Medicine, Shandong University of traditional Chinese Medicine, Jinan 250355 China
[c] Department of Periodontology, Central Laboratory, Jinan Key Laboratory of Oral Tissue Regeneration, Jinan Stomatological Hospital, Jinan 250000 China

*Corresponding authors, e-mail: zyy8965@163.com, xinhongwang325@163.com
† These authors contributed equally to this work.

Received 24 Nov 2025, Accepted 20 Apr 2026
Available online 14 Jun 2026

ABSTRACT: In this study, polysaccharides from *Stropharia rugosoannulata* (*Stropharia rugosoannulata* polysaccharides, SRP) were extracted using aqueous extraction and alcohol precipitation, followed by purification through the Sevag deproteinization method. A radiation-damaged model was established in C57BL/6J mice. The immunomodulatory function and radiation-protective effects of SRP were evaluated using indicators including mouse body weight growth curves, immune organ indices, serum inflammatory factor levels, and histopathological changes in the spleen, thymus, colon, and liver. The results revealed that SRP not only significantly enhanced immune organ indices but also effectively suppressed inflammatory cytokine secretion, mitigating tissue damage in the spleen, thymus, liver, and colon.

KEYWORDS: ionizing radiation, polysaccharides, *Stropharia rugosoannulata*, radiation protection

INTRODUCTION

The radiation produced directly or indirectly by ionizing particles, or by their combination, is called ionizing radiation. With advancements in science and technology, artificial radiation has become widespread across various fields. Studies have demonstrated that the human body's ability to repair radiation damage is limited. Ionizing radiation can lead to radiation diseases, causing lesions in nearly all human organs and systems, and may even result in genetic defects. Currently, amifostine is a widely used radioprotective agent in clinical practice, but it frequently causes symptoms like gastrointestinal dysfunction and hypotension, along with severe toxicity and side effects. Consequently, the development of natural radioprotective agents with low toxicity and minimal side effects is crucial for current radiation protection research.

Polysaccharides, one of the earliest studied natural active products, are abundant in animals, plants, and microorganisms. According to several studies, polysaccharides derived from a variety of animals, plants, and microorganisms exhibit significant biological functions in both daily applications and disease therapy. For instance, they exert protective effects against acute alcoholic liver injury in mice and can serve as active components in cosmeceutical formulations [1, 2]. They are vital components of living organisms and exhibit strong anti-radiation effects [3], making them excellent materials for developing novel radioprotective agents. Thus, a thorough study of the relationship between polysaccharide structure and pharmacological effects is crucial for advancing their development in the medical and food industries.

As a new edible fungus [4], *Stropharia rugosoannulata* is rich in bioactive components, offering substantial nutrition and high medicinal value. Modern pharmacological studies indicate that extracts of *S. rugosoannulata*, particularly its polysaccharides (*S. rugosoannulata* polysaccharides, SRP), exhibit various pharmacological effects such as antibacterial [5, 6], antioxidant [7], anti-tumor [8], hypoglycemic [9], and immune regulation [10, 11]. However, its potential radioprotective effects have not been reported. In the experiment, SRP was extracted using aqueous extraction and alcohol precipitation. A radiation injury model in mice was then developed to evaluate the protective effects of SRP. White blood cell counts, immune organ indices, levels of inflammatory factors, and pathological changes in immune organs were assessed. The spleen tissue was selected for analysis of the mRNA and protein expression of TLR4 and NF-κB p65. The comprehensive evaluation of the protective effects of SRP against radiation injury led to a preliminary understanding of its underlying mechanism.

MATERIALS AND METHODS

Materials and reagents

S. rugosoannulata was sourced from Kunming, Yunnan Province, China. Glacial acetic acid (Analytical grade) was purchased from Shanghai Co., Ltd. (Shanghai,

China). Trypan blue was purchased from Solaibao (Beijing, China). Mouse primary antibody (Batch No. GB15186-50) was purchased from ServiceBio Co., Ltd. (Wuhan, China). Mouse TNF-α ELISA kit (Batch No. YT-0132M1), mouse IL-1β ELISA kit (Batch No. YT-0040M1), and mouse IL-6 ELISA kit (Batch No. YT-0163M1) were purchased from Yutong Biotechnology Co., Ltd. (Jiangsu, China).

Experimental animals

SPF-grade, healthy wild-type C57BL/6J mice, equally distributed by sex, aged 6–8 weeks, and weighing 20 ± 2 g, were sourced from Jinan Pengyue Experimental Animal Breeding Co., Ltd. (Jinan, China), under license SCXK (Lu) 2022-0006. The treatment of all animals in the experiments adhered strictly to the ethical standards of the Laboratory Animal Management and Use Committee of Shandong University of Traditional Chinese Medicine (Ethical Number: SDUTCM20211020001). The temperature of the mouse breeding room was maintained at approximately 24 °C, with proper ventilation, and the mice were provided free access to food and water.

Instruments and equipment

The equipment used in the study includes a rotary evaporator (Zhengzhou Shilian Lianggong Instrument Co., Ltd. (Zhengzhou, China, RE-501), a biological X-ray irradiation instrument (RS2000pro, USA), a high-throughput tissue grinder (XU-YM-24R), a fluorescence microscope (Murzider, MSD520, Mshidi Technology Co., Ltd., Dongguan, China), a frozen centrifuge (Zhejiang Lichen Technology Co., Ltd., Zhejiang, China, LC-LX-HLR210D), an analytical balance (Zhejiang Lichen Technology Co., Ltd., JA1003), a microplate reader (Beijing Pulang Company (Beijing, China, DNM-9602), and a constant temperature incubator (Shanghai Yiheng Scientific Instrument Co., Ltd., Shanghai, China, DHP-9162).

Extraction and purification of SRP

Prior to the formal extraction process, the extraction parameters were optimized using Response Surface Methodology (RSM) based on single-factor experiments. The dried *S. rugosoannulata* was crushed, sieved, and extracted three times under reflux with absolute ethanol, each for 3 h, to remove fat-soluble components. The resulting residue was naturally dried until no alcohol odor remained. The water extraction method was then employed, with two extractions performed for 3 h each. The filtrate was collected and concentrated under reduced pressure. Anhydrous ethanol was added to the concentrated solution, adjusting the ethanol concentration to 80%. The solution was kept at 4 °C for 24 h, then centrifuged and dried. Protein was removed using the Sevag method, and the obtained polysaccharide was redissolved in a suitable amount of distilled water. The polysaccharide solution and the Sevag solution (chloroform:n-butanol = 4:1) were added to a centrifuge tube in a 3:1 ratio, mixed thoroughly for 30 min, and then allowed to stand before centrifugation (5,000 rpm for 10 min) to collect the supernatant. This process was repeated until no protein precipitation was observed between the organic and aqueous phases. After treatment, the supernatant was collected and concentrated under reduced pressure, filtered (3500 D), and finally precipitated with anhydrous ethanol to obtain crude polysaccharides, which were freeze-dried for future use.

The radiation protection effect of SRP

Animal grouping and modeling

Forty healthy, wild-type C57BL/6J mice were randomly divided into five groups: a blank control group (NC), a radiation model group (M), and three groups treated with different doses of SRP (low-dose, SRP-L; medium-dose, SRP-M; high-dose, SRP-H), each with eight mice (half male and half female). The mice were given prophylactic treatment before radiation. The experimental groups were administered *S. rugosoannulata* polysaccharide extract intragastrically, at doses of 100, 400, and 800 mg/kg for the low-, medium-, and high-dose groups, respectively, with a total volume of 0.5 ml. The blank and radiation groups received the same volume of normal saline. The rats were intragastrically administered at a fixed time every day, the body weight was measured every 2 days for 8 days, and the body weight growth curve of mice was plotted. On the 9th day, the mice in the radiation and SRP groups were subjected to a single whole-body X-ray irradiation at a dose of 8 Gy/min, for 4 min and 59 s, at a distance of 100 cm. The blank control group was not irradiated. After 24 h, the mice were euthanized by cervical dislocation while deeply anesthetized with isoflurane via inhalation, and the detection indices were immediately measured.

Determination of whole blood white blood cell count

A total of 20 µl of mouse whole blood was mixed with 0.38 ml of white blood cell diluent (98 ml distilled water, 2 ml glacial acetic acid, and 5 drops of 10 g/ml trypan blue). The white blood cell count was observed using a low-power microscope. The count (N) from four large squares was recorded, and the white blood cell count was determined by calculating $(N/20)\times 10^9$.

Sample collection and processing

The mice were fasted for 12 h before sampling, and their body weights were measured. Blood was collected from the orbit and centrifuged at 3,000 rpm for 10 min. The serum was extracted and stored in a freezer at −20 °C.

Changes of immune organ index

The mice were sacrificed, and their spleen and thymus tissues were collected and weighed. The spleen and thymus indices were calculated using the formula: organ index = (measured organ weight/mouse body weight) × 100%.

Determination of cytokine levels in mouse spleen

Spleen tissue samples were collected, with some preserved for pathological observation. The remaining tissue was homogenized and centrifuged at 3,000 rpm for 15 min to obtain the supernatant. The levels of IL-1β, IL-6, and TNF-α were determined following the ELISA kit instructions.

Pathological observation of spleen, thymus, colon, and liver

The spleen, thymus, colon, and liver tissues of the mice were collected, and any attached blood was blotted away with absorbent paper, while the surrounding adipose tissue was removed. The tissues were fixed with 4% paraformaldehyde solution, and sections of the spleen, thymus, colon, and liver were stained with Hematoxylin and Eosin (H&E). The changes in these tissues for each group were then observed under an optical microscope.

mRNA expression of TLR4 and NF-κB p65 in mouse spleen

Spleen tissue was placed in a mortar, and liquid nitrogen was used to grind the tissue into a fine powder. A 20 mg sample was then taken and mixed with 350 µl of Reservoir Limit Test (RLT) Plus lysis solution in a 1.5 ml EP tube, which was shaken for 20 s to ensure thorough lysis. RNA was extracted using the Cisco Jie RNA extraction kit, and reverse transcription was conducted following the one-step reverse transcription kit protocol in a 20 µl reaction system. All sampling steps were performed on ice, and the resulting cDNA was stored at −20 °C. Primers for the TLR4 and NF-κB p65 genes were designed and synthesized, and the sequences are listed in Table S1 (Supplementary Material). The SYBR Green method was employed to detect the TLR4 and NF-κB p65 genes, and the relative expression of the target gene was calculated using the $2^{-\Delta\Delta Ct}$ method.

Western blot analysis of TLR4 and NF-κB p65 protein expression in mouse spleen

A 100 mg sample of spleen tissue was weighed and transferred to a 1.5 ml Eppendorf (EP) tube, to which 350 µl of protein lysis solution was added. The mixture was homogenized using a grinder and lysed on ice for 30 min and then centrifuged at 12,000 rpm for 10 min. The supernatant was transferred to a new EP tube. Protein concentrations were standardized across all samples using BCA protein quantification, and a 1:4 volume of loading buffer was added. The samples were then heated in a metal bath at 100 °C for 10 min and stored at −20 °C. For electrophoresis, 20 µl of each sample was loaded into the gel wells. The electrophoresis was conducted at 90 V for the stacking gel and 150 V for the resolving gel. After electrophoresis, the proteins were transferred to a Polyvinylidene Fluoride (PVDF) membrane using a 300-mA current for 1 h. The membrane was blocked using fast sealing liquid in a slow shaker for 20 min. It was then incubated with the primary antibody in an antibody incubation box at 4 °C overnight. The PVDF membrane was washed three times with Tris-buffered saline with Tween 20 (TBST), with shaking for 10 min each time. Using tweezers, the membrane was moved to an incubation box containing the secondary antibody and shaken gently for 2 h.

Data analysis

The experimental data were statistically analyzed using GraphPad Prism software (version 8.0), employing the t-test for comparisons. A *p*-value of less than 0.05 or 0.01 was considered statistically significant.

RESULTS

Radiation protection results of SRP

Body weight growth curve of mice

Body weight is a basic index to reflect the physical condition of mice. As shown in Fig. 1a, when the maximum dose of polysaccharides from *S. rugosoannulata* was 800 mg/kg, there was no significant toxic effect in mice. In addition, the mice showed good growth, positive mental state, and good stress response. Their dietary intake, excretion function, and daily behavior patterns were normal, indicating that SRP could be safely evaluated at this dose and could be used for subsequent studies.

The white blood cell counts in the whole blood of mice

When the body is exposed to ionizing radiation, the hematopoietic system is the first to show changes, and a significant early indicator of this damage is a change in peripheral blood [12–14]. The white blood cell count in peripheral blood is an essential indicator for assessing the extent of radiation injury [15]. As shown in Fig. 1b, compared with the NC group, the white blood cell count in the M group was significantly reduced, while the white blood cell counts in the SRP-L, SRP-M, and SRP-H groups were higher than that in the M group. With the SRP-M and SRP-H groups showing statistically significant increases, no significant differences were observed among the remaining groups. The experimental results showed a decrease in white blood cell count in the M group, indicating that radiation significantly affected the blood of mice, inhibiting their hematopoietic function. This study demonstrated that after mice were exposed to X-rays,

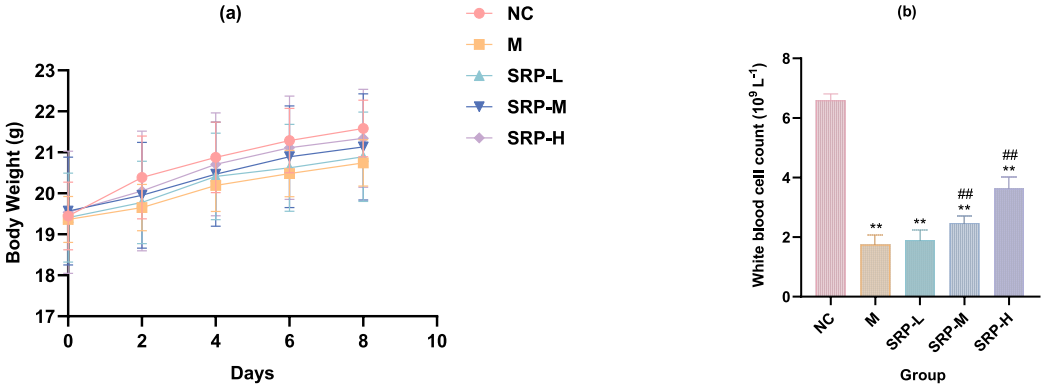

Fig. 1 Body weight growth curves of mice in different treatment groups (a). Effect of different treatment groups on white blood cell counts in irradiated mice ($n = 8$) (b). Note: Compared with the NC group: $^{**}p < 0.01$; compared with the M group: $^{\#\#}p < 0.01$. Blank control group (NC), radiation model group (M), and three groups treated with different doses of SRP (low, SRP-L; medium, SRP-M; high, SRP-H).

the white blood cell count in the peripheral blood of the M group was significantly lower than that in the NC group. After SRP treatment, the white blood cell counts in all SRP groups increased significantly, indicating that SRP had a protective effect on peripheral blood immune cells. This promoted the recovery of the hematopoietic system and enhanced the immune function of mice.

Spleen and thymus indices in mice

The organ index is a reliable metric to evaluate and reflect the physiological status and functional ability of organs [16]. The spleen and thymus are the body's primary immune organs, involved in the maturation and differentiation of immune cells and serving as critical sites for immune responses. Exposure to ionizing radiation can cause varying degrees of damage to these organs, leading to a decrease in their indices [17, 18]. The organ index of mice in each group is shown in Table 1. Compared with the NC group, the spleen and thymus indices of the M, SRP-L, SRP-M, and SRP-H groups were significantly decreased, indicating that radiation caused acute damage to the immune organs in mice. However, compared with the M group, the spleen and thymus indices in the SRP-L, SRP-M, and SRP-H groups were increased and positively correlated with the dose. With the SRP-M and SRP-H groups showing statistically significant increases, no significant differences were observed among the remaining groups. The results of this experiment showed that SRP effectively improved the immune activity of the mice, alleviated radiation-induced damage to immune organs, and exhibited protective effects against radiation.

Serum levels of IL-1β, IL-6, and TNF-α in mice

As shown in Fig. 2, the levels of IL-1β, IL-6, and TNF-α in the M group increased to varying degrees compared with the NC group. After pre-treatment with SRP, the levels of IL-1β, IL-6, and TNF-α in the treated groups significantly decreased compared with the radiation group, with the difference being statistically significant. This indicates that SRP can mitigate the radiation-induced inflammatory response in mice.

Histopathological sections

The results of H&E staining of spleen tissue are presented in Fig. 3a. In the blank group, the white and red pulp of the spleen were evenly distributed. In the irradiation model group, the red pulp increased, cells were loosely arranged and vacuolated, and inflammatory infiltration was present. In comparison to the irradiation model group, the white pulp significantly increased and was evenly distributed across each dose group, indicating an increase in lymphocytes and clear boundaries.

The results of H&E staining of thymus tissue are shown in Fig. 3b. In the blank group, thymocytes were neatly arranged, and the boundary between the cortex and medulla was distinct. The cortex primarily consisted of lymphocytes and thymic epithelial cells with densely packed lymphocytes. The medulla was lightly stained, mainly composed of numerous thymic epithelial cells and a few lymphocytes, showing round or oval thymic corpuscles of varying sizes. In the irradiation model group, vacuolar degeneration of thymic epithelial cells was observed in the medulla area, where the intercellular space expanded, and inflammatory cell infiltration appeared. In comparison to the irradiation model group, improvements were observed gradually from the low-dose to the high-dose groups, with the cell boundaries becoming clear and the morphology appearing normal across all dose groups.

The results of liver histological examination using H&E staining are presented in Fig. 3c. In the control group, hepatic lobules exhibited normal architecture with radially arranged hepatic cords, absence of con-

Table 1 Effects of different treatment groups on organ indices of mice after radiation.

Group	NC	M	SRP-L	SRP-M	SRP-H
Spleen index (mg/g)	34.05 ± 14.11	13.04 ± 1.65**	13.06 ± 2.16**	15.22 ± 2.96**	20.75 ± 2.43$^{**,\#\#}$
Thymic index (mg/g)	23.28 ± 6.07	3.93 ± 1.31**	4.48 ± 0.97**	8.31 ± 0.96**	14.36 ± 1.77$^{**,\#\#}$

The data in the table are presented as mean ± standard deviation ($n = 8$); compared with the NC group, $^{**}p < 0.01$; compared with the M group, $^{\#\#}p < 0.01$. Blank control group (NC), radiation model group (M), and three groups treated with different doses of SRP (low, SRP-L; medium, SRP-M; high, SRP-H).

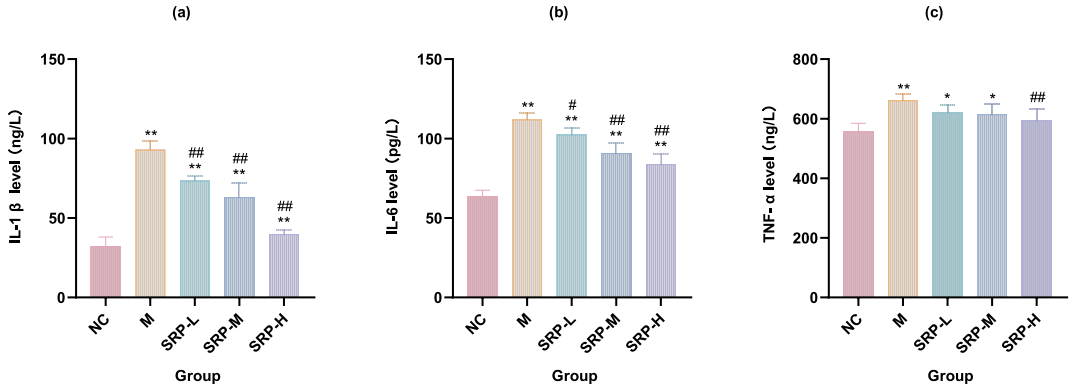

Fig. 2 Effects of different treatment groups on serum levels of IL-1β, IL-6, and TNF-α in mice: IL-1β (a), IL-6 (b), and TNF-α (c). Note: Compared with the NC group: $^{*}p < 0.05$, $^{**}p < 0.01$; compared with the M group: $^{\#}p < 0.05$, $^{\#\#}p < 0.01$. Blank control group (NC), radiation model group (M), and three groups treated with different doses of SRP (low, SRP-L; medium, SRP-M; high, SRP-H).

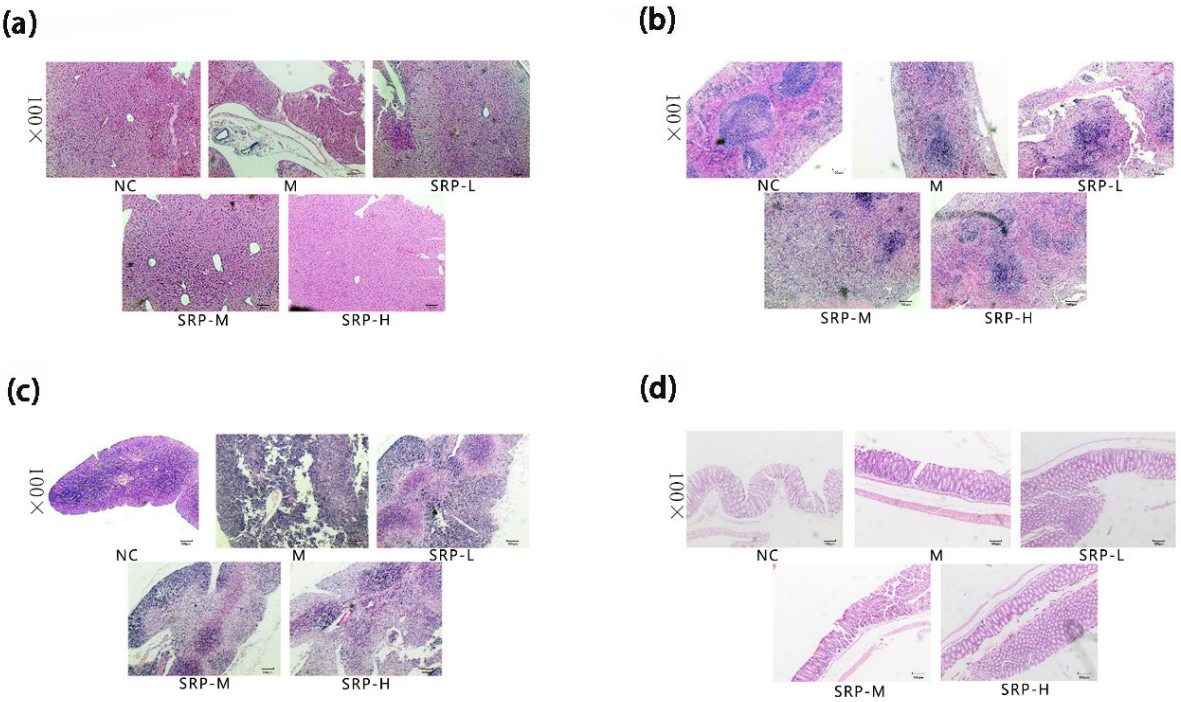

Fig. 3 Histopathological sections of the spleen (a), thymus (b), liver (c), and colon (d) of mice in different treatment groups (100×). Blank control group (NC), radiation model group (M), and three groups treated with different doses of SRP (low, SRP-L; medium, SRP-M; high, SRP-H).

gestion, inflammatory cell infiltration, and clear outlines of hepatocytes. In contrast, the irradiation model group showed enlarged liver cell interstitium, disordered arrangement of hepatic cords, and infiltration of inflammatory cells. In the low-dose group, there was slight restoration of liver cell interstitium and hepatic cord structures, along with reduced inflammatory cell infiltration compared with the irradiation model group. The medium-dose group demonstrated significant restoration of liver cell interstitium and hepatic cord structures with some remaining inflammatory cell infiltration. In the high-dose group, the liver cell interstitium and hepatic cord structures were close to normal.

The results of H&E staining of colon tissue are illustrated in Fig. 3d. In the control group, the morphological structure of colon cells appeared normal without any signs of inflammatory infiltration. Conversely, in the radiation group, numerous inflammatory cells infiltrated the colons of the mice, resulting in altered cell morphology and disrupted cellular structure. In the low-dose group, there was a reduction in inflammatory cell infiltration, albeit with altered cell morphology, while the overall cellular structure remained relatively intact. In the medium-dose group, inflammatory cell infiltration was infrequent, and the cell morphology was close to normal. In the high-dose group, occasional inflammatory cell infiltration was observed, with cell morphology appearing normal.

mRNA expression of TLR4 and NF-κB p65 in the colon of mice

The experimental findings are depicted in Fig. 4a and b. Compared with the NC group, the mRNA expression levels of TLR4 and NF-κB p65 were markedly elevated in the M group. Conversely, compared with the M group, the treatment group exhibited significantly reduced mRNA expression of TLR4 and NF-κB p65. These results indicate that SRP effectively inhibits the expression of TLR4 and NF-κB p65 in colon tissues, thereby exerting an anti-radiation inflammatory response.

TLR4 and NF-κB p65 protein expression in colon tissues

As illustrated in the Fig. 4c and d, the protein expression levels of TLR4 and NF-κB p65 were significantly elevated in the M group compared with the NC group. Conversely, compared with the M group, the treatment group exhibited markedly reduced protein expression levels of TLR4 and NF-κB p65. These findings suggest that SRP can modulate the protein levels of TLR4 and NF-κB p65 to exert an immune-regulatory role.

DISCUSSION

Recent studies have demonstrated that radiation exposure can induce dose-related damage to various organs in the body. These injuries include a decrease in the number of peripheral blood immune cells, damage to immune organs, and inflammatory responses [19, 20]. An increasing body of literature has highlighted the radioprotective effects of mushroom polysaccharides. For instance, lentinan has been shown to enhance the production of NO and IL-2 by regulating T lymphocytes, consequently improving the viability and function of these cells and enhancing lentinan's anti-radiation efficacy [21, 22]. Tremella polysaccharides have been found to regulate thioredoxin-interacting protein and thioredoxin reductase 2, thus mitigating skin cell damage caused by ultraviolet radiation [23]. Yu et al [24] demonstrated that *Ganoderma lucidum* polysaccharides significantly ameliorated peripheral blood cell counts, potential biomarkers, and metabolic pathways in irradiated mice. Pillai et al [25] showed that β-glucan (BG) isolated from *G. lucidum* polysaccharides notably enhanced the survival rate of irradiated mice and mitigated immune cell damage.

The spleen and thymus are vital immune organs in the body. The organ indices of the thymus and spleen serve as indicators reflecting the body's immune function. Both the thymus and spleen are highly sensitive to radiation and are susceptible to damage from ionizing radiation. In addition to these primary immune organs, other adjacent target organs such as the liver and colon are also impacted by radiation. The results demonstrate that SRP can enhance immune organ indices and mitigate immune organ damage, thus confirming the efficacy of SRP in alleviating radiation-induced immunosuppression and providing certain radiation protection effects.

Toll-like receptors (TLRs) constitute an essential class of protein molecules crucial for non-specific immunity, serving as a bridge between non-specific and specific immune responses. Among them, TLR4 stands out as a member of the TLR family with the remarkable ability to recognize pathogens, transmit diverse activation signals, and actively participate in the body's immune defense mechanisms [26]. On the other hand, NF-κB, functioning as a protein complex and a pivotal transcription factor for inflammation-related genes, exerts control over DNA transcription upon activation, thereby orchestrating the production of downstream inflammatory cytokines and playing a significant regulatory role in the cascade of inflammatory factors [27]. During the inflammatory response, various pathogen-associated molecular patterns (PAMPs) activate the TLR4/NF-κB signaling pathway, prompting the transcription of downstream inflammation-related genes. This cascade leads to the secretion of cytokines such as IL-1β, IL-6, and TNF-α, ultimately resulting in inflammatory injury within the body [28]. Building upon the aforementioned theoretical foundation, in addition to organ index determination and pathological analysis, this study utilized spleen tissue as a representative sample to evaluate the expression of key molecules within the TLR4/NF-κB signaling pathway in mice

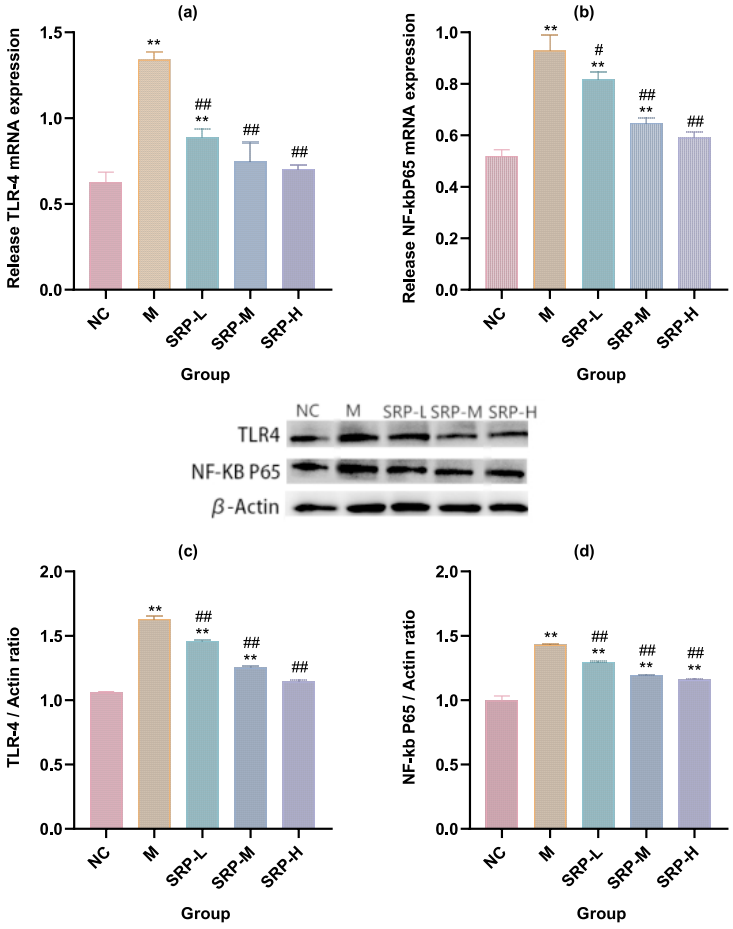

Fig. 4 mRNA expression levels of TLR4 (a) and NF-κB p65 (b) in mouse colon tissues of different treatment groups. Protein expression levels of TLR4 (c) and NF-κB p65 (d) in mouse colon tissues of different treatment groups. TLR4 (a): compared with the NC group, $^{**}p < 0.01$; compared with the M group, $^{\#\#}p < 0.01$; NF-κB p65 (b): compared with the NC group, $^{**}p < 0.01$; compared with the M group, $^{\#}p < 0.05$, $^{\#\#}p < 0.01$. TLR4 (c): compared with the NC group, $^{**}p < 0.01$; compared with the M group, $^{\#\#}p < 0.01$; NF-κB p65 (d): compared with the NC group, $^{**}p < 0.01$; compared with the M group, $^{\#\#}p < 0.01$. Blank control group (NC), radiation model group (M), and three groups treated with different doses of SRP (low, SRP-L; medium, SRP-M; high, SRP-H).

from each group. The results obtained through ELISA, PCR, and Western blot techniques demonstrated that SRP significantly decreased the expression of inflammatory factors IL-1β, IL-6, and TNF-α in radiation-injured mice. Furthermore, SRP also reduced the mRNA and protein expression levels of TLR4 and NF-κB p65, indicating its potential role in radiation protection through the modulation of the TLR4/NF-κB pathway. Specifically, SRP achieves this by inhibiting the expression of upstream key molecules like TLR4 and NF-κB, thereby reducing the levels of downstream inflammatory factors.

In summary, SRP demonstrates the ability to increase the number of peripheral blood leukocytes and immune organ indices, facilitate organ repair, inhibit key molecules within the TLR4/NF-κB signaling pathway, and reduce the expression of inflammatory factors such as IL-1β, IL-6, and TNF-α. Consequently, SRP effectively mitigates the inflammatory response induced by radiation. These findings not only offer a theoretical foundation for the advancement and utilization of *S. rugosoannulata* but also contribute to the exploration of radiation protection strategies. Additionally, they provide a theoretical reference for the further development of radiation protection agents.

Appendix A. Supplementary data

Supplementary data associated with this article can be found at https://dx.doi.org/10.2306/scienceasia1513-1874.2026.051.

Acknowledgements: This research was funded by the National Natural Science Foundation of China (No. 82374311), the Natural Science Foundation of Shandong Province (No. ZR2020MH395), and the key Research and Development Program Foundation of Shandong Province (No. 2022CXGC020514). I would like to express my sincere grat-

itude to my supervisor, Professor Zhang, for his invaluable guidance and continuous support throughout this research.

REFERENCES

1. Chen L, Huang L (2024) Protective effect and mechanisms of *Chimonanthus salicifolius* polysaccharide on acute alcoholic liver injury in mice. *ScienceAsia* **50**, 2024112.
2. Srisukchayakul P, Werasura T, Teeravet S, Pradapphai P, Kannika A, Muangman T, Ayudthaya SPN, Suwannachart C (2024) Development of β-glucan production from microorganisms as active ingredients in cosmeceutical products for skin youthfulness. *ScienceAsia* **50**, 2024045.
3. Ding Y, Cui L, Hua MM, Zhang YM, Guo GB, Sun R, Chen BY (2014) Protective effect of angelica sinensis polysaccharide and astragalus polysaccharides on radiation injury in mice model of compatibility. *Mil Med J Southeast China* **16**, 572–574.
4. Li ZP, Li Y, Zhou F (2018) Industrial culture technology of *Stropharia rugosoannulata*. *Edible Fungi* **40**, 49–50.
5. Wang H, Chen H, Zhang J (2018) Research progresses on bioactive components in *Stropharia rugosoannulata* and their pharmacological effects. *Acta Edulis Fungi* **25**, 115–120.
6. Wei L, Jing B, Li X (2021) Evaluation of nutritional ingredients, biologically active materials, and pharmacological activities of *Stropharia rugosoannulata* grown under the bamboo forest and in the greenhouse. *J Food Qual* **2021**, 5478227.
7. Jia J, Xie XC, Song Y (2021) Optimizing culture medium and antioxidant activity of extracellular polysaccharides in liquid fermentation of *Stropharia rugosoannulata*. *Northern Horticulture* **24**, 105–115.
8. Singh RS, Kaur HP, Kanwar JR (2016) Mushroom lectins as promising anticancer substance. *Curr Protein Pept Sci* **17**, 797–807.
9. Zhai X, Zhao A, Geng L (2013) Fermentation characteristics and hypoglycemic activity of an exopolysaccharide produced by submerged culture of *Stropharia rugosoannulata* #2. *Ann Microbiol* **63**, 1013–1020.
10. Wu YL, Feng WY, Zhang LY (2020) Extraction of polysaccharide from *Stropharia rugosoannulata* and its effect on immunity of mice. *Food Nutr China* **26**, 50–53.
11. Zhou X (2019) Effects of polysaccharides from *Stropharia rugosoannulata* on spleen immune function and p-p38MARK protein expression in overexercising rats. *J Yangzhou Univ (Agric Life Sci)* **40**, 71–75.
12. Chen YB, Chai M, Wu LHS, Han Y (2017) Radiation-induced injury classification, manifestation and mechanism. *Chin J Injury Repair (Electron Ed)* **12**, 203–206.
13. Wang K, Shao X (2021) Analysis of the hazards and protection of ionizing radiation. *Shihezi Sci Technol* **1**, 29–30.
14. Saadat E, Alireza M, Hamed M, Mohammad K (2021) Assessment of some factors of cellular and humoral immunity in radiology workers. *Radiat Environ Biophys* **3**, 411–419.
15. Wang A, Wang Y, Shi ZY (2020) Acute radiation injury caused by 2 Gy 60Co γ ray in mice and the protective effects of a prescription of Chinese medicine. *World J Integr Tradit West Med* **15**, 1049–1053.
16. Li WJ, Li L, Zhen WY, Wang LF, Pan M, Lv JQ, Wang F, Yao YF, et al (2017) *Ganoderma atrum* polysaccharide ameliorates ROS generation and apoptosis in spleen and thymus of immunosuppressed mice. *Food Chem Toxicol* **99**, 199.
17. Cao JY, Chu JJ, Cao J (2013) Pharmacodynamic effect of Sanli capsule on radiation-damaged mice. *Pharm Serv Res* **13**, 150–152.
18. Jin H, Wang DW, Peng RY, Wang SM, Gao YB, Wen-Hua HU, Wang XM, Wang CE, et al (2004) Pathological study on immune organ damage in mice after electromagnetic pulse radiation. *Bull Acad Mil Med Sci* **28**, 537–540.
19. Ito R, Hale LP, Geyer SM, Li J, Sornborger A, Kajimura J, Kusunoki Y, Yoshida K, et al (2017) Late effects of exposure to ionizing radiation and age on human thymus morphology and function. *Radiat Res* **187**, 589–598.
20. Kapoor V, Collins A, Griffith K, Ghosh S, Wong N, Wang X, Challen GA, Krambs J, et al (2020) Radiation induces iatrogenic immunosuppression by indirectly affecting hematopoiesis in bone marrow. *Oncotarget* **11**, 1681–1690.
21. Markova N, Kussovski V, Drandarska I, Nikolaeva S, Georgieva N, Radoucheva T (2003) Protective activity of Lentinan in experimental tuberculosis. *Int Immunopharmacol* **3**, 1557–1562.
22. Wang Y, Li MC, Fu QJ (2013) Protective effects of lentinan against T lymphocytes injury in mice under chronic radiation stress. *Chin Herb Med* **5**, 62–66.
23. Lin M, Bao C, Chen L (2023) *Tremella fuciformis* polysaccharides alleviates UV-provoked skin cell damage via regulation of thioredoxin interacting protein and thioredoxin reductase 2. *Photochem Photobiol Sci* **22**, 2285–2296.
24. Yu C, Fu J, Guo L, Lian L, Yu D (2020) UPLC-MS-based serum metabolomics reveals protective effect of *Ganoderma lucidum* polysaccharide on ionizing radiation injury. *J Ethnopharmacol* **258**, 112814.
25. Pillai TG, Uma DP (2013) Mushroom beta glucan: potential candidate for post irradiation protection. *Mutat Res* **751**, 109–115.
26. Crammond P, Hastak P, Delaney A, Sasson SC (2026) Taking its TOLL: the role of toll-like receptor 4 in human health and disease, and its potential as a therapeutic target. *Front Immunol* **17**, 1761361.
27. Nishida A, Andoh A (2025) The role of inflammation in cancer: Mechanisms of tumor initiation, progression, and metastasis. *Cells* **14**, 488.
28. Yuan Y, Li CY, Toliken A, Chen Y, Yao YH, Zhao J (2026) Protective effects of licochalcone A against alcoholic liver injury in mice by modulating the gut-liver axis and TLR4/NF-κB pathway. *Foods* **15**, 915.

Appendix A. Supplementary data

Table S1 Primer sequences.

Gene	Sequence
TLR-4	Forward Primer CGCTCTGGCATCATCTTCATTGTC Reverse Primer CCTCCCATTCCAGGTAGGTGTTTC
NF-κB	Forward Primer ATGGGAAACCGTATGAGCCTGTG Reverse Primer AGTTGTAGCCTCGTGTCTTCTGTC
β-Actin	Forward Primer GTGCTATGTTGCTCTAGACTTCG Reverse Primer ATGCCACAGGATTCCATACC